

**SPE/DOE 24192**

**Gel Placement in Heterogeneous Systems With Crossflow**

**K.S. Sorbie, Heriot-Watt U., and R.S. Seright, New Mexico Petroleum Recovery Research Center**

SPE Members

Copyright 1992 Society of Petroleum Engineers Inc

This paper was prepared for presentation at the SPE/DOE Eighth Symposium on Enhanced Oil Recovery held in Tulsa, Oklahoma April 22-24, 1992

This paper was selected for presentation by an SPE Program Committee following review of information contained in an abstract submitted by the author(s). Contents of the paper as presented, have not been reviewed by the Society of Petroleum Engineers and are subject to correction by the author(s). The material as presented does not necessarily reflect any position of the Society of Petroleum Engineers, its officers, or members. Papers presented at SPE meetings are subject to publication review by Editorial Committees of the Society of Petroleum Engineers. Permission to copy is restricted to an abstract of not more than 300 words. Illustrations may not be copied. The abstract should contain conspicuous acknowledgment of where and by whom the paper is presented. Write Librarian Manager SPE, P.O. Box 833836, Richardson TX 75083-3836 Telex 730989 SPEDAL

**ABSTRACT**

Early water breakthrough can be a serious problem during waterflooding of heterogeneous reservoir formations. One possible remedy to this problem is to place a gel block in the high-permeability layer, thus diverting displacing brine into the less-permeable layers in order to sweep the remaining oil from these zones. In such a treatment, the gelant material must be placed in the correct location within the reservoir so that gel does not *impair* reservoir performance. In this paper, we study the dynamics of gel placement in heterogeneous (stratified) reservoir systems. The details of the gel placement are strongly affected by the level of communication between reservoir layers, which is characterized by the closeness of the system to vertical equilibrium (VE) conditions. We show that in viscous-stable injection of gelant in systems close to vertical equilibrium, considerable volumes of injected material can crossflow into the low-permeability layers, and subsequent gel formation can seriously reduce the performance of the continuing waterflood. Results from a range of experimental displacements in well characterized layered beadpacks are presented, along with supporting numerical simulations, which help to understand the mechanisms and benefits when performing gel treatments in reservoir systems with free crossflow. The central role of viscous crossflow in such systems is demonstrated. Since we consider only viscous forces in this work, the layered experimental packs are scaled only by the viscosity ratio (displacing to displaced), the geometry of the packs,

the aspect ratio and the degree of vertical communication (closeness to VE). Thus the conclusions from the experimental and simulation results are directly applicable to similarly scaled viscous-dominated systems at the reservoir scale. Some analysis is also presented of the mechanism of disruption of slugs by viscous fingering in layered systems.

**INTRODUCTION**

The objective of gel treatments in injection wells is to reduce flow through fractures or high-permeability zones while diverting injected fluids into hydrocarbon-bearing strata. In oil production wells, the main objective of gel treatments is to reduce water production without significantly reducing oil production. Achieving these objectives may be impeded by the formation of gel material in less-permeable, oil-productive zones.<sup>1-4</sup> If gel treatments are to improve sweep efficiency, a pathway must be available between the wellbore and mobile oil in the formation. This can sometimes be accomplished by mechanically isolating zones during the gel treatment. However, zone isolation will not be effective if extensive crossflow can occur between reservoir layers of contrasting permeability (or possibly, if flow can occur behind pipe).

Much of the previous work concerning gel placement has focused on gel treatments in reservoirs with no communication between zones.<sup>1-4</sup> However, crossflow can occur to some extent in most reservoirs<sup>5</sup>; therefore, a need exists to

---

References and illustrations at end of paper

characterize the effect of crossflow on gel placement. Previous workers<sup>6-8</sup> investigated crossflow of water and oil downstream of the gel-treated region. In contrast, this paper focuses on the impact of crossflow during the process of the gel placement. Crossflow concepts from previous studies<sup>9-17</sup> are applied with the objective of placing a gel such that sweep efficiency can be improved in stratified reservoirs with some degree of vertical communication between strata.

To visualize the effects of crossflow on gel placement, we have performed a series of experiments in large, scaled beadpacks which contain up to four contrasting permeability layers. These floods were followed by direct visualization since plexiglass models were used. These experiments are analyzed using a combination of simple analytical models and direct numerical simulation in order to clarify the main features of the gelant placement mechanism and the subsequent recovery after a successful (or an unsuccessful) gel placement.

### CONCEPT OF GELANT PLACEMENT, POSTFLUSH AND GELATION

**Basic Concept.** The basic idea to be examined in this section is illustrated schematically in Fig. 1. During waterflood operations, assume that injected water has reached a production well by following a high-permeability pathway. For the first step of the gel treatment, a gelant with a water-like viscosity is injected (Fig. 1a). Because of the low viscosity of the gelant, penetration into the less-permeable zones is minimized.<sup>1,3</sup> Secondly, water is injected to displace the water-like gelant away from the wellbore (Fig. 1b). Sufficient water must be injected so that the rear of the gelant bank in the most-permeable zone outruns the front of the gelant bank in an adjacent less-permeable zone. In the third step of the process (Fig. 1c), the well is shut in to allow gelation to occur. Finally, if the gel treatment is applied in a waterflood injection well, water injection is resumed. Hopefully, a pathway will be available for water to crossflow from the high-permeability zone into the less-permeable zone(s) so that sweep efficiency can be improved (Fig. 1d).

If this scheme is feasible, then it could provide favorable injectivity characteristics. During water injection after gelation, much of the water leaving the wellbore should enter the most-permeable zone. Contrary to the objectives in systems with no crossflow between layers, it is **not** desirable for the gel treatment to cause more water to leave the wellbore directly into the low-permeability strata. If

the cross-sectional area is relatively large in the region where water crossflows from the high-permeability zone into the low-permeability zone (Fig. 1d), then injectivity losses from the gel treatment could be minimized (particularly for unfractured injection wells, where flow is radial). In contrast, conventional gel treatments (i.e., those with no postflush prior to gelation) in unfractured injection wells should cause significant injectivity losses.<sup>1</sup>

The "incremental" oil from this scheme could be recovered relatively quickly. As shown in Fig. 1d, oil displaced from the less-permeable zones can crossflow into the most-permeable zone, where it can flow more rapidly to the production well.<sup>10</sup> Of course, this idea may be applied to production wells, to injection wells in CO<sub>2</sub> floods, steam floods, and other enhanced oil recovery processes, as well as to waterflood injection wells.

**Limitations.** A number of limitations should be recognized for this scheme. First, the gel treatment will not improve sweep efficiency beyond the greatest depth of gelant penetration in the reservoir when there is fluid crossflow between layers.<sup>6</sup> Once beyond the gel bank in the most-permeable zone, fluids can crossflow back into the high-permeability channel.

Gelation time is an important factor that limits the depth of gelant penetration in a reservoir. In concept, many variables (e.g. temperature, pH, salinity, and gelant composition) could be manipulated to achieve virtually any desired gelation time. If the gel treatment is confined to the region near the wellbore, then these variables may be useful in controlling gelation. However, if the gelant is to penetrate a significant distance into the reservoir, then control of gelation time is usually quite limited. Under reservoir conditions, gelation times for common oilfield gelants are relatively short (0 to 10 days, typically; perhaps a few weeks in special cases). If the offending channel is a very conductive fracture, then a typical gelant could penetrate a large distance into the reservoir before gelation occurs. However, if the channel consists of a very permeable rock matrix, then very long gelation times (months to years) may be needed in order to achieve large depths of gelant penetration<sup>7</sup>. (The different requirements for fractures vs. matrixes arise primarily because of their substantial differences in both permeability and pore volume). Thus, there may be a need for a new low-viscosity gelants with very long gelation times.

One very important limitation that will emerge later in this paper is that the viscosity and resistance factor of the gelant must not be too large. For such cases, it will be shown that viscous gelant will penetrate to a greater degree into the less-permeable zones. Furthermore, prior to gelation, viscous gelants will crossflow continuously from the high-permeability channel into the adjacent less-permeable zones.<sup>10,12</sup> This creates a barrier of viscous gelant in the less-permeable zones all along the interface with the high-permeability channel. When a water postflush is injected, the barrier hinders crossflow of water from the high-permeability channel into the less-permeable zones. Thus, viscous fingers from a water postflush will break through the viscous gelant bank in the high-permeability channel before breakthrough in less-permeable zones. This can render the process ineffective; further discussion of this effect is presented below.

The remainder of this paper will attempt to demonstrate the above points and to define how viscous the gelant can be while still allowing the overall concept illustrated in Fig. 1 to work.

## VERTICAL EQUILIBRIUM AND CROSSFLOW BETWEEN LAYERS

In this paper, we will first contrast the depth of gelant penetration in stratified systems both with and without the possibility of fluid crossflow between the strata. We will then examine the redistribution of gelant during a water postflush prior to gelation. Finally, the flow distribution will be examined during water injection after gelation. We demonstrate that the efficacy of the gel placement depends critically on whether the displacement is "understable" or "overstable". An *understable* displacement is defined by Eq. 1.

$$F_r < \frac{k_1}{k_2} \quad (1)$$

where  $k_1$  is the permeability of a high-permeability stratum,  $k_2$  is the permeability of an adjacent less-permeable zone, and  $F_r$  is the resistance factor for the gelant which is defined as the mobility of the fluid displaced by the gelant divided by the mobility of the gelant. In the absence of permeability reduction during the gel placement step, then  $F_r$  is simply the ratio of the injected-fluid (gelant) viscosity to that of the in-situ-fluid viscosity; this is the case in most of our displacement experiments but is not generally true in the field where an adsorbing, pore blocking gelant is usually employed.

In the same way, an *overstable* displacement is defined by Eq. 2.

$$F_r > \frac{k_1}{k_2} \quad (2)$$

If crossflow can occur between layers or flow paths in a reservoir, viscous fluids (specifically, fluids with a lower mobility than that of the fluid that is being displaced) will penetrate into low-permeability layers to a greater extent than if crossflow is not possible. This has been demonstrated by a number of researchers<sup>5,10-12,15,17</sup>, and it can be illustrated further by considering a linear, two-layer, horizontal reservoir as shown inset in Fig. 2. The effective aqueous-phase porosities for the more-permeable layer (Layer 1) and the less-permeable layer (Layer 2) are denoted as  $\phi_1$  and  $\phi_2$ , respectively. Assume that water is initially the only mobile fluid in the region of interest and a viscous, Newtonian, water-miscible fluid is injected to displace the resident water. For simplicity, gravity, capillary forces, and dispersion are neglected in this treatment, and all experimental results presented are for miscible fluid displacements.

**No-Crossflow Case:** During gelant injection, we are interested in the relative positions of the gelant-water fronts in the two layers,  $L_{p2}/L_{p1}$ , where  $L_{p1}$  and  $L_{p2}$  are the depths of penetration of the gelant in Layers 1 and 2, respectively (see inset Fig. 2). For the case where there is zero vertical flow between the layers, analytical solutions for the ratio,  $L_{p2}/L_{p1}$ , are readily available.<sup>1</sup> In particular, Eq. 3 describes  $L_{p2}/L_{p1}$  for a viscous Newtonian fluid in a linear flow system at the time when the injected gelant reaches the end of the most-permeable layer<sup>1</sup>:

$$\frac{L_{p2}}{L_{p1}} = \frac{\sqrt{1 + (F_r^2 - 1) \left[ \frac{\phi_1 k_2}{\phi_2 k_1} \right]} - 1}{F_r - 1} \quad (3)$$

The predicted curve for  $L_{p2}/L_{p1}$  in a no-crossflow case as a function of  $F_r$  is shown in Fig. 2 for a permeability contrast of 10:1 (where  $\phi_1 = \phi_2$ ). The above formula predicts that, assuming  $\phi_1 = \phi_2$ , the frontal advance ratio,  $L_{p2}/L_{p1}$ , approaches  $(k_2/k_1)^{1/2}$  as  $F_r$  is increased. This is an interesting result in itself since, injecting a viscous material for "heterogeneity control"<sup>17</sup> in a system with no crossflow, will *at best* increase  $L_{p2}/L_{p1}$  to  $(k_2/k_1)^{1/2}$ . For example, if  $k_2/k_1 = 1/100$  in the linear no-crossflow system, then the frontal advance

ratio ( $L_{p2}/L_{p1}$ ) could only be reduced to 1/10, even with an infinite-viscosity displacing fluid

**Free-Crossflow Case:** At the other extreme from the zero-crossflow case, vertical permeability between layers is very large and conditions of vertical equilibrium (VE) exist.<sup>13-16</sup> Vertical equilibrium is associated with large values of the following "shape" scaling group:

$$G_{\text{shape}} = \frac{k_z}{k_x} \cdot \left[ \frac{\Delta x}{\Delta z} \right]^2 \quad (4)$$

where ( $k_z/k_x$ ) is the ratio of the vertical to horizontal permeability and  $A_x$  and  $A_z$  are the total length and height of the system, respectively. VE implies that the horizontal pressure gradients are equal at all vertical positions at a particular longitudinal position along the reservoir. Attainment of vertical equilibrium depends on two main factors, the ratio of vertical to horizontal permeability and the reservoir aspect ratio.<sup>15,16</sup> However, vertical equilibrium is generally a valid assumption for reservoirs with effective length-to-width ratios greater than ten if no barriers to vertical flow exist and it has been analyzed in terms of the  $G$  group presented above.<sup>15,18</sup> Of course, for the case of no vertical crossflow,  $G_{\text{shape}} = 0$ .

If vertical equilibrium applies and if the displacement is understable ( $F_r < k_1/k_2$ ), then the ratio of frontal velocities ( $v_2/v_1$ ) is approximated by Eq. 5 for gelant injection into our linear two-layer reservoir.<sup>14,19</sup>

$$\frac{v_2}{v_1} \approx \frac{\phi_1 k_2 F_r}{\phi_2 k_1} \quad (5)$$

Similarly, if vertical equilibrium is applicable at all times, the relative positions of the injectant-water fronts in the two layers are approximated by Eq. 6.

$$\frac{L_{p2}}{L_{p1}} \approx \frac{\phi_1 k_2 F_r}{\phi_2 k_1} \quad (6)$$

If vertical equilibrium applies, and if the displacement is overstable ( $F_r > k_1/k_2$ ), then Eq. 6 appears to suggest that the ratio,  $L_{p2}/L_{p1}$ , is greater than unity (i.e. the advancement of the front in the lower permeability layer is faster than that in the higher permeability layer). In reality, as vertical equilibrium is approached, this ratio *tends to unity* as the displacement becomes overstable. That is, the fronts in adjacent layers can be almost coincident in an overstable displacements, and the ratio of frontal velocities ( $v_2/v_1$ ) is approximately equal to 1.<sup>15</sup>

However, the gelant front in Layer 2 will always lag somewhat behind the front in Layer 1 because vertical equilibrium cannot be fully attained. These conclusions, which imply that the frontal shape becomes asymptotically fixed in viscous overstable displacements, are confirmed experimentally by the results presented in this work and elsewhere.<sup>12</sup>

The top curve (with  $G_{\text{shape}} \rightarrow \infty$ ) in Fig. 2 predicts  $L_{p2}/L_{p1}$  as a function of resistance factor for the case where vertical equilibrium exists between the layers. As expected,  $L_{p2}/L_{p1}$  has the same value with or without crossflow if the resistance factor of the viscous fluid is equal to one.<sup>5,12</sup> In other words,  $L_{p2}/L_{p1} = k_2/k_1$  when  $F_r=1$ . If  $F_r > 1$ , then  $L_{p2}/L_{p1}$  is greater with crossflow than without crossflow.

If the vertical permeability between the layers is finite, then the  $L_{p2}/L_{p1}$  values will be greater than those for the case with no crossflow but less than those for the case of vertical equilibrium. This is illustrated by the curves calculated numerically using a fairly fine grid structure (80x10) for intermediate values of  $G_{\text{shape}}$  (0.01, 10 and 20000) in Fig. 2 for a permeability ratio of  $k_1/k_2 = 1/10$ . At very low values of crossflow ( $G_{\text{shape}} = 0.01$ ), the frontal advance ratio agrees very well with the theoretical formula for the no-crossflow case (Eq. 3 above), and we also note that the errors in locating the fronts in the two layers are relatively small. In Fig. 2, note that the calculated  $L_{p2}/L_{p1}$  curve for  $G_{\text{shape}}=0.01$  appears to fall below the no-crossflow theoretical case. In reality this cannot happen. As suggested by the error bars for the  $G_{\text{shape}}=0.01$  curve, this anomaly is due to the error in locating the fronts during the numerical simulation. When very high levels of crossflow can occur ( $G_{\text{shape}} = 20000$ ), we expect the system to approach the VE case shown in Fig. 2. Indeed, it does give a reasonable approximation to this case, but there are errors associated with pinpointing the exact location of the fronts in each layer when there is free crossflow. These errors are not a numerical dispersion effect but are due to the way the viscous stable fronts are spread vertically in such cases, as shown experimentally in Fig. 3a and in our numerical results (e.g., see Fig. 4). The error bars in the ratio  $L_{p2}/L_{p1}$  arising from this effect are shown in Fig. 2 for all the numerical calculations. An intermediate crossflow case ( $G_{\text{shape}} = 10$ ) is also shown in Fig. 2. We note that the relevant value of the shape scaling group for a given gel treatment in the field need not mean that the entire well to well distance be taken as  $A_x$ . If, for example, the gel treatment extends 100 ft into a formation 10 ft thick and  $k_z/k_x = 0.1$ , then the appropriate  $G_{\text{shape}}$  would be 10. If a deeper gel placement was attempted *in the same*

*formation*, to a distance of 500 ft, then  $G_{\text{shape}}$  would be 250, and crossflow would be *more important*. Alternatively, if the gel treatment was limited to within 10 ft of the well in the same formation, then  $G_{\text{shape}} = 0.1$ , and crossflow may not be very important.

Analyses have been made using the vertical equilibrium concept including gravity, capillary forces, multiphase flow, dispersion, and other effects.<sup>13-16,18</sup> These analyses confirm that  $L_{p2}/L_{p1}$  for viscous injectants will generally be greater with crossflow than without crossflow. Since viscous gelants can penetrate farther into less-permeable zones with crossflow than without crossflow, it follows that when these gelants form gels, low-permeability zones can experience more damage in reservoirs with crossflow than in those where crossflow is not possible.

## VISCOUS CROSSFLOW DURING GELANT PLACEMENT

**Experimental and Numerical Verification Using Newtonian Fluids.** The effects of crossflow in a viscous overstable displacement are illustrated in Fig. 3 where comparison is made with a corresponding unit mobility displacement in layered Pack 1 (Table 1). These experiments use dye labelled brine and glycerol in layered beadpacks held within plexiglass containments; the floods are visualized and imaged as shown in Fig. 3. The properties of the two layer pack used in these experiments are held within given in Table 1, and further details of the construction and packing are presented elsewhere.<sup>12</sup> The main feature of the two-layer system (Pack 1) is that the permeability contrast is approximately 5:1 and the viscosity ratio is 8:1 ( $F_v = 8$ ) in the viscous overstable displacement. Substantial crossflow has clearly occurred for the overstable displacement, indicating an unsatisfactory placement of the fluid viscous in Fig. 3a. Fig. 3(b) shows that the unit mobility placement is much more satisfactory. The case with unit mobility ratio represents the most optimistic situation that can be achieved since there is zero crossflow (apart from a small amount of fluid redistribution close to the injector since all injection is into the high permeability layer).

The levels of crossflow during the placement of viscous material into the layered system may be illustrated using numerical simulation. Results for several viscosities of "gelant" are shown in Fig. 4. This figure shows both the position of the viscous material after a 0.4 PV slug was injected and the

levels of crossflow calculated directly in the simulation using the sector-sector flow option of the simulator. As expected, the level of crossflow is greatest for the most viscous injectants. Once the viscous-overstable limit is exceeded, a fixed degree of crossflow occurs. This viscous crossflow mechanism has been analyzed theoretically<sup>15</sup> and has been discussed in the context of polymer flooding for "heterogeneity control".<sup>9,10,17</sup>

**Experimental Verification Using Xanthan Solutions.** Additional experiments were conducted by injecting xanthan solutions to displace water from a two-layer beadpack (Pack 2; Table 1). One layer of Pack 2 was 11.2 times more permeable than the other layer. Again, dyed fluids (water and xanthan solution) were injected to allow visualization of crossflow. The displacing fluids used in these floods contained between 0-ppm and 2000-ppm xanthan. Viscosity values at  $11 \text{ s}^{-1}$  range from 1 cp to 75.2 cp and are listed in Table 2. The injection rate was maintained at 200 ml/h and all fluids had approximately the same density, thus minimizing the effects of gravity. This was verified by repeating floods with the high- and low- permeability layers inverted; no differences were observed in the frontal displacement patterns. All floods in the beadpacks were repeated several times in order to establish reproducibility. Rheological information (viscosity vs. shear rate) for the xanthan solutions and additional details of these experiments can be found in Ref. 19.

The experimental results are illustrated in Fig. 5 and Table 2. These experiments demonstrate that the degree of crossflow into the less-permeable layer increases with increased viscosity of the displacing fluid (xanthan solution). When the polymer/water viscosity ratio was greater than the permeability ratio (i.e., as for the 1000-ppm and 2000-ppm xanthan solutions), the average velocity for the polymer fronts was approximately equal in both layers (see Table 2). This observation is in accordance with the theoretical predictions discussed above for the near-vertical-equilibrium limit. These results are also in very good agreement with those presented earlier for Newtonian fluids.<sup>12</sup>

Additional analysis which considers the non-Newtonian nature of the xanthan solutions used in these floods can be found in Ref. 19 and some important conclusions from that analysis are as follows:

1. For conventional polymer solutions, the ratio of frontal velocities,  $v_2/v_1$ , will never be less than the value attained for an injectant with  $F_r$

- = 1. This assumes that other factors are equal; in particular, chemical retention, density, and the permeability dependence of  $F_r$  for the injectants being compared are the same.
2. As injection rate is increased, the ratio of frontal velocities,  $v_2/v_1$ , should decrease for shear-thinning fluids, increase for shear-thickening fluids, and remain unaffected for Newtonian fluids, assuming that gravity and capillary forces are negligible compared with viscous forces. Different rate dependencies can be observed if gravity and capillary forces are important, even for Newtonian fluids.<sup>5, 12</sup>
  3. For shear-thinning fluids, an injection profile measured at the wellbore might suggest that an unexpectedly high fraction of the fluid enters the most-permeable zone. This might mislead one to *incorrectly* conclude that shear-thinning fluids penetrate a lesser distance into low-permeability zones than will water-like fluids.

In summary, we note that, if crossflow can occur, viscous gelants can enter and damage less-permeable, oil-productive zones more than if crossflow is not possible. In unfractured injection wells where extensive crossflow can occur between strata, a polymer flood, which is intended for "heterogeneity control"<sup>17</sup>, will be favored over a gel treatment that uses a viscous gelant. To consider this point further, for either a near-producer gel treatment or an in-depth gel treatment, we must now consider attempts to displace a viscous slug away from the wellbore region.

## THE GELANT-SLUG POSTFLUSH

**Experimental Demonstration Using Newtonian Fluids.** In order to examine the next stage of the gel placement (Fig. 1b), we compare the propagation of a unit-mobility and a viscous-overstable slug away from the well (see Fig. 6). Fig. 6 shows the effect of a brine postflush for the same cases as are shown in Fig. 3 (Pack 1). The unit-mobility case gives a desirable placement of the model gelant (Fig. 6a). For the viscous case, however, the model viscous gelant is placed extensively in the low-permeability zone. A more complete analysis of the dynamics of the viscous slug breakdown is presented in Ref. 12. Ref. 12 demonstrates that viscous fingers may form in the earlier stages of the postflush because an adverse mobility ratio exists. Finger formation in stratified

systems will be discussed in more detail later in this paper. However, we conclude that the best possible placement that can be achieved when crossflow is present is obtained by using a unit-mobility gelant.

**Experimental Demonstration Using Xanthan Solutions.** After injecting the xanthan solutions as indicated in Fig. 5, water was injected to determine where viscous fingers from the water postflush would first break through the polymer bank. The results are summarized in Table 3 for four different xanthan solutions and are illustrated in Fig. 7 specifically for the case with 2000-ppm xanthan. The experiments demonstrated that in systems with crossflow, viscous fingers from a water postflush virtually always break through the viscous bank first in the most-permeable layer. Additional details of these experiments can be found in Ref. 19 and very similar results were found for Newtonian fluids in Ref. 12. The idea of fingering through a viscous slug in a layered system is considered further below and in Appendix A.

## Benefits from a Unit-Mobility Gelant.

Two issues remain to be considered for heterogeneous (layered) systems with free crossflow:

- (i) What benefits can be gained in terms of additional recovery when we use a unit-mobility gelant placement?  
and
- (ii) How viscous a gelant can we actually use and still retain an acceptable placement of the gelant even though some crossflow will occur?

The second point is important since gelant material in practice will often be more viscous than brine and so the maximum acceptable gelant viscosity must be established. From the discussion above, the gelant/brine viscosity ratio,  $F_r$  (in the absence of permeability reduction), must be less than the permeability ratio,  $k_1/k_2$ . Thus, the injection must be *understable*, but we must establish *how* unstable. Both of the above issues will be dealt with below using a combination of displacement experiments in stratified packs and numerical simulation.

In order to demonstrate the benefits of a unit-mobility gelant placement in a layered system, a two-layer beadpack with a high to low-permeability ratio of 5:1 was used. The high-permeability layer thickness was half that of the low-permeability layer (Pack 3; Table 1). A unit-mobility continuous flood with dyed brine displacing colorless brine is shown

at a series of times in Figs. 8a-8e. As expected, the displacement efficiency is poor. The corresponding recovery for the unit-mobility flood as a function of pore volume throughput is shown in Fig. 9. The recovery in Fig. 9 is taken directly from the images of the flood. Due to the mixing zone definition in the floods in the plexiglass containment, the error is approximately  $\pm 0.03$  (PV) on the scale of the figure shown.

A corresponding unit-mobility gel placement experiment was performed in Pack 3 pack using a gelant formulation that formed a very solid gel. This gelant formulation contained 4000-ppm HE-300® synthetic polymer (produced by Phillips), 10500-ppm formaldehyde and 5250-ppm resorcinol. The gelant had a viscosity of  $\approx 48$  cp before setting, and in the conditions within the pack, required about 3 days to fully set at ambient conditions. We emphasize here that this is *not* a practical formulation for a field application due to the high viscosity and high concentrations of the various components, nor is it the type of formulation that is intended by the manufacturers of the HE product. This gelant formulation was used with in situ and postflush "brines" of 48 cp such that the effective placement and postflush periods simulated a unit-mobility case as discussed above. This was also demonstrated for purely neutral (non gelling) fluids in Fig. 6 above. The gelant placement stage is illustrated in Figs. 8f and 8g. After gelant placement, the system was subsequently shut in for 3 days (the gelation time). After that time, the gelant formed a fairly solid gel in both the high- and the low-permeability layers. The postflush period is shown for the unit-mobility (i.e. 48 cp) brine in Figs. 8h to 8j. The throughput values (in PV) associated with Figs. 8a-8e are almost the same as those in Figs. 8f-8j, respectively. The recovery efficiencies for these two floods (neutral and gelling) are compared directly in Fig. 9. The displacement efficiency is indeed better at the same injected fluid throughput (compare Figs. 8d and 8i and Figs. 8e and 8j). Fig. 9 indicates that, at 1 PV total fluid injection, the recovery efficiency is substantially greater for the gel treated system than for the unit-mobility flood. The slight discrepancy in the early period of both floods (between 0 and 0.4 PV) is due to the error in estimating the recovery (as discussed earlier).

#### LIMITATIONS ON GELANT VISCOSITY FOR EFFECTIVE PLACEMENT IN SYSTEMS WITH CROSSFLOW

**Experiments in Four-Layer Packs.** We have demonstrated that the best gelant placement is

obtained when the process is at unit mobility. This is not usually practical for polymer-crosslinker gelant materials where the viscosity is often considerably above that of brine. Other types of gelants can have a low initial viscosity<sup>20-24</sup>. The question therefore arises: how viscous can the gelant be before crossflow and propagation problems lead to an unsatisfactory placement? The answer will depend on the permeability contrast between the thief zone and adjacent layers. Certainly, the ratio,  $F_r k_2/k_1$ , must be less than unity, but we need to know *how large* this quantity can be and still obtain an acceptable gel placement.

To demonstrate this in a system with a number of strata, the results from miscible viscous-slug-placement experiments are presented in four-layer beadpacks. Two similar packs (Packs 4 and 5) were used that had wide permeability contrast (ranging over a factor of 100). These packs are described in Table 1. In these packs, two important permeability contrasts are (1) the contrast between the highest- and next-highest-permeability layers ( $-37$  and  $-29$  for Packs 4 and 5, respectively), and (2) the contrast between Layer 1 and the least-permeable layers (Layers 3 and 4, where  $k_1/k_3$  and  $k_1/k_4$  are both  $-150$  and  $-100$  for Packs 4 and 5, respectively). The viscous slugs had  $F_r$  values of 2.96 and 15.3, respectively, so the  $F_r k_2/k_1$  ratios were 0.08 and 0.53 in Packs 4 and 5, respectively. For all floods, the viscous fluids and the postflush "brine" were injected only into the most-permeable layer.

The flood profiles for the initial viscous slug placement and the subsequent postflush period are presented in Figs. 10 and 11. In these figures, the (enhanced) scanned images are shown along with an inset sketch to assist interpretation. In Fig. 10, where the system is very understable,  $F_r k_2/k_1 = 0.08$ , the "gelant" placement appears to be quite satisfactory. However, there is still some degree of crossflow from Layer 1 to Layer 2 both during the initial placement of the slug and during the postflush period. There is also some degree of fingering/mixing at the rear of the slug during the postflush period. Fig. 11 shows an understable case for Pack 5 where  $F_r k_2/k_1 = 0.53$ . Clearly, there is significantly more "gelant" crossflow in this case, both during the initial placement and postflush periods. The fingering at the rear of the slug is also much more severe, as expected for a local mobility ratio of 15.3 (i.e.  $\mu_p/\mu_w = 92$  cp/ 6 cp), and leads to the rapid disintegration of the viscous "gelant" slug. Thus, the value of  $F_r k_2/k_1 = 0.53$  is probably too high for a successful treatment in this system.

Figs. 10 and 11 show that, for each of the viscous "gelant" placements, different conclusions may be reached concerning how well the treatment assists oil recovery in the *very low* permeability layers (Layers 3 and 4) where the permeability contrast with Layer 1 is  $> 100:1$ . Whereas, the "gelant" placement in Fig. 10 was very satisfactory in terms of the additional sweep of adjacent layer 2 ( $(k_1/k_2) = 36.8$ ), *only* Layer 2 will benefit from this treatment. If we wished to improve the sweep from the remaining layers in Pack 4, then a further gelant treatment would be required. In contrast, the more viscous "gelant" used in the treatment in Pack 5 ( $F_r k_2/k_1 = 0.53$ ) did not give a satisfactory placement in terms of improving the recovery from Layer 2.

**Demonstration Using Simulation.** In order to support the conclusions from our experimental results, we present a number of results from the numerical simulation of unit-mobility and viscous gel placement in a layered system and the subsequent recoveries obtained. The simulation model assumes a simple three-layer system with a high-permeability central region with a thickness of 0.18 of the system height and a 10:1 permeability contrast with the rest of the reservoir. The two less-permeable layers are of equal thickness (0.41 of the system thickness), and the overall aspect ratio of the system is  $(\Delta x/\Delta z) = 10$ . Since we expect the local  $(k_z/k_x)$  to be very close to unity, the value of the shape group is,  $G_{\text{shape}} = 100$  and we therefore expect the system to be quite close to VE. A fine grid (80x40) is used in the simulations with the high permeability region being represented by a 80x30 grid. A fine grid is required in the high-permeability streak since, during the postflush stage, there will almost certainly be some fingering at the rear of the viscous gelant slug. As we noted during our experiments, fingering will occur almost entirely in the high permeability layer and this is also found in direct numerical simulations.<sup>12</sup> Incidentally, in any simulation of gel placement, a sufficiently fine grid is also very important in the low-permeability layers - especially near the wellbore.

In the calculations, we follow the procedures listed below and make the following assumptions:

- (i) the gelant material is a purely viscous fluid during injection into the reservoir (i.e. there is no adsorption, permeability reduction, non-Newtonian rheology etc.) and is injected miscibly; therefore,  $F_r$  is essentially the ratio of gelant viscosity to displaced brine viscosity.

- (ii) after placement, the permeabilities in the region where the "gelant" resides (after the postflush) are reduced by a factor of 100, irrespective of the layer involved.
- (iii) the postflush is essentially unit mobility and "sees" the modified permeability field according to point (ii) above.

The simulations described in this work, have two distinct stages. The first is the placement of gelant, including the (possibly unstable) brine postflush. The second stage is the continued period of brine injection after the simple permeability reduction following the notional gel-formation period. Fig. 12 shows the position of the gelant in the system just prior to the shutin period where the gel will set; this figure shows the regions where the permeability reduction will take place as described in (ii) above. The placement phase is satisfactory for the unit-mobility and, possibly, the  $F_r = 2$  cases. However, because of the levels of viscous crossflow, the placement appears much less satisfactory for the higher viscosity cases. Since only viscous forces are involved here, the conclusions are valid for any system with the same geometry, and values of  $G_{\text{shape}}$ ,  $k_1/k_2$  and  $F_r$ . The placement efficiency shown in Fig. 12 is further supported by the values of recovery (of in situ fluid) as a function of PV injected. Fig. 13 indicates that a gelant viscosity giving a  $F_r$  value up to 2 (i.e. a ratio of  $F_r k_2/k_1$  of 0.2) is acceptable, but as  $F_r$  increases to 5 ( $F_r k_2/k_1 = 0.5$ ) the performance is degraded quite significantly. We suggest that the ratio  $F_r k_2/k_1$  may reach  $\approx 0.3$  and still yield a satisfactory gel placement and subsequent recovery performance, but should not exceed this value in systems with free crossflow.

Caution should be used when interpreting Figs. 12c through 12e. In these cases, the brine postflush broke through the gelant banks first in the central high-permeability layer. Although not apparent in these figures, a layer of gel exists at the interface between the high- and low-permeability zones. This layer of gel inhibits the brine postflush from crossflowing behind the rear of the gel bank from the high-permeability zone into the adjacent less-permeable zones. Instead, brine from the postflush continues to finger through the gelant in the high-permeability layer. This is not accounted for in our simple numerical model which should, therefore, give optimistic oil recovery results.

Note that the more viscous treatments shown in Fig. 13 provide better recovery values than the straightforward unit-mobility flood. However, this has little to do with the gel formation and is principally due to the additional improved recovery

that arises from the crossflow (from the low to the high-permeability layer) during the initial placement of the viscous gelant. This recovered "oil" from the low-permeability layer crossflows into the high-permeability layer during the viscous-overstable placement from whence it is ultimately produced. This is essentially the "heterogeneity control" mechanism that operates in polymer flooding (without gelation) in highly heterogeneous systems that has been referred to above.<sup>17</sup>

### FINGERING AT REAR OF GELANT SLUG

One aspect of the gelant placement problem which is clearly very important is the degree of fingering that occurs at the rear of a viscous slug in a layered system where there is free crossflow. Thus, at vertical equilibrium, the placement/postflush problem involves the following two parts:

- (i) the viscous-stable displacement at the front of the slug where the velocity of the front in the high-permeability layer depends on both the permeability contrast and the resistance factor i.e. on  $F_r k_1/k_2$ .
- (ii) the unstable advance of the finger at the rear of the viscous slug where, experimentally, virtually all of the fingering is observed in the high-permeability layer<sup>12</sup>, and the frontal advance velocity depends only on the mobility ratio (i.e.  $F_r$ , if the postflush and in situ brines are the same and there is no permeability reduction).

From these considerations, we have derived a simple formula in Appendix A for the "dimensionless slug breakdown ratio",  $t_p/t_s$ , which can be used to give an estimate of when the finger will breakthrough in the high-permeability layer during the gelant postflush. The quantity,  $t_p$ , is the slug size (in PV) of the postflush of lower viscosity fluid that just breaks through a gelant slug of size,  $t_s$ . The various steps in the process are illustrated schematically in Fig. 14 and the details are presented in Appendix A. The formula for  $t_p/t_s$  derived in Appendix A has been applied to the xanthan-slug-breakdown data discussed above. The results from the xanthan experiments are presented in Table 4 and Fig. 15. It can be seen from Fig. 15 that the formula in Eq. A7 gives a reasonable estimate of  $t_p/t_s$  for breakdown in layered systems where VE applies. However, in order to assess the generality applicability of these results, further work will be necessary.

### CONCLUSIONS

In this paper, we have addressed the problem of performing gel treatments in heterogeneous stratified systems where there is some degree of crossflow between layers. The main conclusions from the experimental and simulation results are as follows:

- (i) The degree of crossflow, or "closeness" to vertical equilibrium (VE), is governed by the value of the shape group (Eq. 4). This allows the conclusions reported here to be applied to field systems with approximately the same geometry, permeability contrast ( $k_1/k_2$ ),  $F_r$  and  $G_{shape}$ . For the no-crossflow case,  $G_{shape} = 0$  and, as  $G_{shape} \rightarrow \infty$ , the system approaches VE.
- (ii) In the presence of crossflow in an unfractured, layered heterogeneous reservoir system, it is very desirable to have a unit-mobility gelant where  $F_r = 1$  (i.e. a fluid with essentially brine viscosity).
- (iii) If crossflow between strata can occur, then viscous gelants can enter and damage less-permeable, oil-productive zones to a greater extent than if crossflow cannot occur.
- (iv) For viscous *overstable* gelant slugs in systems with free crossflow, both the original placement of the material and the subsequent propagation away from the well are very unsatisfactory due to the extent of the viscous crossflow that occurs. During the postflush period, much of the viscous gelant may finally reside in the low-permeability strata where gel may form and damage sweep efficiency. However viscous crossflow has a beneficial effect during a polymer flood, where the central aim is "heterogeneity control" in the reservoir<sup>17</sup>.
- (v) In practice, some degree of viscosity of the gelant can be "tolerated" although this must still give a viscous *understable* displacement in the initial stages to reduce crossflow to acceptable levels. We suggest an approximate practical guideline for gelant placement in systems with crossflow is to maintain  $F_r k_2/k_1 \leq 0.3$ .
- (vi) Fingering at the rear of the viscous gelant slug will occur during the period when gelant is propagated away from the well by the brine postflush. When there is relatively free fluid crossflow in a layered system, this will occur

mainly in the high-permeability layer and will be accompanied by crossflow of the viscous material into the less-permeable layer. A simple approximate formula (Eq. A7) has been proposed to estimate when slug breakdown will occur. However, the precise severity of this fingering in a real reservoir situation is not accurately assessable from our experimental floods or numerical calculations and more work must be carried out to investigate this issue.

## NOMENCLATURE

$F_r$	= resistance factor (mobility of the displaced reservoir fluids divided by mobility of the injected viscous fluid); for a miscible flood without permeability alteration, $F_r$ is simply the ratio of displacing to displaced fluid viscosity i.e $F_r = (\mu_p/\mu_w)$ .
$G_{shape}$	= dimensionless "shape" scaling group defined in Eq. 4
$k_i$	= effective permeability to water for Layer i, md [ $\mu m^2$ ]
$k_z, k_x$	= vertical and horizontal permeability respectively, md [ $\mu m^2$ ]
$L_{pi}$	= length of the gelant bank in Layer i, ft [m]
$L$	= system length, ft [m]
$t_s, t_p$	= time or size in PV of injected gelant slug or postflush at slug breakdown respectively
$v_i$	= fluid velocity in Layer i, ft/d [m/s]
$\beta$	= dimensionless constant in Eq. AS given by, $\beta = (\Delta z_1 \phi_1) / (\Delta z_2 \phi_2)$ .
$\mu_p$	= viscosity of the gelant or polymer solution, cp [mPa-s]
$\mu_w$	= water viscosity, cp [mPa-s]
$\phi_i$	= effective aqueous-phase porosity in Layer i
$\Delta z_i$	= effective layer thickness of Layer i
$\Delta x, \Delta z$	= system total length and thickness respectively, ft [m]
$\omega$	= Todd and Longstaff mixing parameter

## ACKNOWLEDGMENTS

The authors would like to thank the following colleagues: A. Hosseini, M. Sheb and F. Feghi of Heriot-Watt University for their assistance with the

experimental and computational work. At the New Mexico Petroleum Recovery Research Center, we thank J. C. Hagstrom for performing beadpack studies and J. Liang and H. Greder for helpful discussions. RSS also thanks the following for financial support: The U.S. Department of Energy, Conoco, Elf Aquitaine, Marathon Oil, Mobil Research and Development, Oryx Energy, Phillips Petroleum, Shell Development, and Texaco. KSS thanks Mobil (North Sea) Ltd. for their generous support of the experimental work at Heriot-Watt University and for the advice and technical support of Dr R Seetharam of Mobil (Dallas Research Laboratories).

## REFERENCES

1. Seright, R.S.: "Placement of Gels to Modify Injection Profiles," paper SPE/DOE 17332 presented at the 1988 SPE/DOE Enhanced Oil Recovery Symposium, Tulsa, April 17-20.
2. Liang, J., Lee, R.L., and Seright, R.S.: "Placement of Gels in Production Wells," paper SPE/DOE 20211 presented at the 1990 SPE/DOE Enhanced Oil Recovery Symposium, Tulsa, April 22-25.
3. Seright, R.S.: "Effect of Rheology on Gel Placement," *SPE* (May 1991) 212-218.
4. Seright, R.S.: "Impact of Dispersion on Gel Placement for Profile Control," *SPE* (Aug. 1991) 343-352.
5. Craig, F.F., Jr.: *The Reservoir Engineering Aspects of Waterflooding*, Society of Petroleum Engineers, Dallas (1971) 62-76.
6. Root, P.J. and Skiba, F.F.: "Crossflow Effects During an Idealized Displacement Process in a Stratified Reservoir," (Sept. 1965) *SPEJ* 229-237.
7. Scott, T. *et al*: "In-Situ Gel Calculations in Complex Reservoir Systems Using a New Chemical Flood Simulator," *SPE* (Nov. 1987) 634-646.
8. Gao, H.W. *et al*: "Studies of the Effects of Crossflow and Initiation Time of a Polymer Gel Treatment on Oil Recovery in a Waterflood Using a Permeability Modification Simulator," paper SPE/DOE 20216 presented at the 1990 SPE/DOE Symposium on Enhanced Oil Recovery, Tulsa, April 22-25.

9. Clifford, P.J. and Sorbie, K.S.: "The Effects of Chemical Degradation on Polymer Flooding," paper SPE 13586 presented at the 1985 SPE International Symposium on Oilfield and Geothermal Chemistry, Phoenix, April 9-11.
10. Sorbie, K.S. and Clifford, P.J.: "The Simulation of Polymer Flow in Heterogeneous Porous Media in *Water-Soluble Polymers for Petroleum Recovery*, G.A. Stahl and D.N. Schulz (eds.), Plenum Press, New York (1988) 69-99.
11. Sorbie, K.S. *et al.*: "Miscible Displacements in Heterogeneous Core Systems: Tomographic Confirmation of Flow Mechanisms," paper SPE 18493 presented at the 1989 SPE International Symposium on Oilfield Chemistry, Houston, Feb. 8-10.
12. Sorbie, K.S. *et al.*, "Scaled Miscible Floods in Layered Beadpacks Investigating Viscous Crossflow, the Effects of Gravity and the Dynamics of Viscous Slug Breakdown", paper SPE 20520 presented at the 1990 SPE Annual Fall Conference, New Orleans, LA, Sept. 23-26.
13. Coats, K.H. *et al.*: "Simulation of Three-Dimensional, Two-Phase Flow in Oil and Gas Reservoirs," (Dec. 1967) *SPEJ* 377-388.
14. Coats, K.H., Dempsey, J.R., and Henderson, J.H.: "The Use of Vertical Equilibrium in Two-Dimensional Simulation of Three-Dimensional Reservoir Performance," *SPEJ* (March 1971) 63-71.
15. Zapata, V.J. and Lake, L.W.: "A Theoretical Analysis of Viscous Crossflow," paper SPE 10111 presented at the 1981 SPE Annual Technical Conference and Exhibition, San Antonio, Oct. 5-7.
16. Dake, L.P.: *Fundamentals of Reservoir Engineering*, Elsevier Scientific Publishing Co., New York, (1978) 349-428.
17. Sorbie, K.S., *Polymer Improved Oil Recovery*, CRC Press, Boca Raton, Florida, USA, (1991).
18. Yortsos, Y.C. : "A Theoretical Analysis of Vertical Flow Equilibrium", paper SPE 22612, presented at the 1991 SPE Annual Fall Conference, Dallas, TX, Oct. 6-9.
19. Seright, R.S. and Martin, F.D.: "Fluid Diversion and Sweep Improvement with Chemical Gels in Oil Recovery Processes," second annual report (DOE/BC/14447-10), U.S. DOE (Nov. 1991) 86-110.
20. McLaughlin, H.C., Diller, J. and Ayres, H.: "Treatment of Injection and Producing Wells with Monomer Solution," paper SPE 5364 presented at the 1975 SPE Regional Meeting, Oklahoma City, Mar. 24-25.
21. Felber, B.J. and Dauben, D.L.: "Development of Lignosulfonate Gels for Sweep Improvement," paper SPE 6206 presented at the 1976 Annual Fall Technical Conference and Exhibition, New Orleans, Oct. 3-6.
22. Jurinak, J.J., Summers, L.E. and Bennett, K.E.: "Oilfield Application of Colloidal Silica Gel," paper SPE 18505 presented at the 1989 SPE International Symposium on Oilfield Chemistry, Houston, Feb. 8-10.
23. Seright, R.S. and Martin, F.D.: "Impact of Gelation pH, Rock Permeability, and Lithology on the Performance of a Monomer-Based Gel," paper SPE 20999 presented at the 1991 SPE International Symposium on Oilfield Chemistry, Anaheim, Feb. 20-22.
24. Fletcher, A.J.P. *et al.*: "Deep Diverting Gels for Very Cost Effective Waterflood Control," Proceedings of the Sixth European Symposium on Improved Oil Recovery, Stavanger (May 21-23, 1991), 329-335.
25. Todd, M.R. and Longstaff, W.J., "The Development, Testing and Application of a Numerical Simulator for Predicting Miscible Flood Performance", Trans. AIME, Vol. 253, (July 1972) 874-882.
26. Sorbie, K. S., Tsibuklis, N. B. and Dwebi, A., "Experimental Testing of Mobility Predictions in Averaged Models of Viscous Fingering", paper SPE 22617, presented at the 1991 SPE Annual Fall Conference, Dallas, TX, Oct. 6-9.

## APPENDIX A

## Finger Breakthrough Time in Displacements in Layered Systems

For the case of free crossflow (at VE) in a layered system then, for an understable displacement (where  $\phi_1 = \phi_2$ )

$$\frac{L_{p2}}{L_{p1}} \approx \frac{k_2 F_r}{k_1} \quad (\text{A1})$$

If the two layers are of equal thickness then

$$\frac{L_{p1} + L_{p2}}{2L} = t_s \quad (\text{A2})$$

where  $t_s$  is the injected gelant slug PV for the first stage of the placement. Using the above equations and rearranging gives:

$$\frac{L_{p1}}{L} = \frac{2 t_s}{\left( \frac{k_2 F_r + 1}{k_1} \right)} \quad (\text{A3})$$

Note that this describes the *linear* advancement with time of the front in the high-permeability layer as shown schematically in Fig. 14a. Suppose we now miscibly inject a brine postflush mobility ratio,  $M = F_r$ . This brine will initially finger into the gelant slug in the high-permeability layer (as shown in Fig. 14b), forming a finger of length  $L_f$ , which grows *linearly* with time. Using the Todd and Longstaff model<sup>25</sup> for the fingering process within Layer 1, an "averaged" finger growth rate<sup>26</sup> is estimated as follows:

$$\left( \frac{L_f}{L} \right) = a t \quad (\text{A4})$$

where  $t$  is time in PV and the constant  $a$  is given, in this case, by:

$$\alpha = M^{1-\omega} = F_r^{1-\omega} \quad (\text{A5})$$

where  $\omega$  is an empirical mixing parameter<sup>25</sup> and we use the velocity of the tip of the finger where the effective displacing fluid concentration is approximately zero. In this work, we use  $\omega = 2/3$  in all calculations although this quantity may vary with system aspect ratio. Further tuning of this parameter will be investigated in more detail in future work.

Recent experimental evidence suggests that the Todd and Longstaff method is an appropriate model for describing fingering in such systems<sup>26</sup>.

The question now arises: when, approximately, will the finger in the postflush "catch" the front of the gelant in the high permeability region? This situation is shown in Fig. 14c after the injection of  $t_p$  pore volumes of postflush, where clearly  $L_f = L_{p1}$ . At this point, we may equate Eqs. A3 and A4 to obtain:

$$\left( \frac{L_{p1}}{L} \right) = \frac{2}{\left( \frac{k_2 F_r + 1}{k_1} \right)} (t_s + t_p) = 2 F_r^{1-\omega} \cdot t_p \quad (\text{A6})$$

which easily rearranges to give us the ratio of gelant slug/postflush brine pore volumes,  $(t_p/t_s)$ , at which the fingering will just reach the front as in Fig. 14c. This expression is given by:

$$\left( \frac{t_p}{t_s} \right) = \frac{1}{\left( \frac{k_2 F_r + 1}{k_1} \right) F_r^{1-\omega} - 1} \quad (\text{A7})$$

Eq. A7 for the "dimensionless slug breakdown ratio",  $(t_p/t_s)$ , makes physical sense since the gelant advancement in the high-permeability layer ( $L_{p1}$ ) depends on the quantity,  $F_r k_2/k_1$ . However, the advancement rate of the finger ( $L_f$ ) depends on the mobility ratio ( $F_r$  in this case) but not the permeability ratio. A limitation of Eq. A7 is the VE assumption. In particular, as the slug placement becomes overstable, ( $F_r > (k_1/k_2)$ ), then the quantity  $F_r k_2/k_1$  must be set to unity in Eq. A7. A comparison of experimental results for xanthan slug breakdown with Eq. A7 is shown in Table 4 and Fig. 15 ( $\omega = 2/3$ ). Note that, in Fig. 15, there are considerable errors in the experimental points due to uncertainties in the estimate of the in situ (porous medium) xanthan shear rate which has a very strong effect on the polymer viscosity. At higher concentrations, xanthan solutions are very shear thinning. However, there is reasonable overall agreement between the experimental data and the simple theoretical formula of Eq. A7.

**Table 1: Properties of Layered Beadpacks Used in Flow Experiments**

	Pack 1		Pack 2		Pack 3		Pack 4				Pack 5			
	Layer 1	Layer 2	Layer 1	Layer 2	Layer 1	Layer 2	Layer 1	Layer 2	Layer 3	Layer 4	Layer 1	Layer 2	Layer 3	Layer 4
Length in Flow Direction (cm)	56		238		55.8		55.8				55.8			
Width (cm)	1.3		1.3		1.3		1.3				1.3			
Total Height (cm)	5.8		11.6		6.3		12				12			
Layer thickness (cm)	2.9	2.9	5.8	5.8	2.1	4	2	3	3	3	3	3	3	3
Nominal bead diameter or range ( $\mu\text{m}$ )	75-150	45-90	500	150	75-150	45-90	400-520	75-150	45-90	0-40	400-520	75-150	45-90	0-40
Approx. Layer Permeability (Darcies)	-5	-1	152	13.6	-5	-1	-150	-5	-1	-1	-150	-5	-1	-1
$k_1/k_2$ ( $k_3/k_4$ ) ratio	5:1		11.2:1		5:1		173 : 4.7 : 1.3 : 1.0 $k_1/k_2 = 36.8$				100 : 3.4 : 1.04 : 1.0 $k_1/k_2 = 29.4$			
Porosity	0.38	0.38	0.38	0.38	0.36	0.36	0.36	0.36	0.36	0.36	0.36	0.36	0.36	0.36
$G_{shape}$ (Assuming $k_x = k_z$ )	93.2		421		78.4		21.6				21.6			

Table 2. Summary of beadpack experiments with xanthan; status at the end of polymer injection

	Xanthan concentration, ppm				
	0	200	500	1000	2000
Number of trials	6	9	7	4	7
Xanthan solution viscosity, cp @ $11 \text{ s}^{-1}$ , $25^\circ\text{C}$	1.0	3.1	8.2	23.3	75.2
Average final relative position of fronts, $L_{p2}/L_{p1}$	0.095	0.223	0.586	0.835	0.915
Average final relative velocity of fronts, $v_2/v_1$	0.085	0.225	0.644	0.974	0.993

Table 3. Summary of Beadpack Experiments with Xanthan, Status when fingers from water postflush break through the xanthan bank in the high-permeability layer

	Xanthan concentration, ppm			
	200	500	1000	2000
Number of trials	7	6	4	7
Average postflush volume + polymer solution volume	3.4	1.12	0.47	0.20
Length of postflush front or longest finger in low-k layer + polymer bank length in low-k layer	0.70	0.09	0.054	0.014
Average final relative position of polymer fronts, $L_{p2}/L_{p1}$	0.116	0.540	0.874	0.939

Table 4: Experimental data and theoretical predictions for the dimensionless slug breakdown ratio for the xanthan floods in Pack 2

Experiment	Resistance Factor $^1 F_r$	Ratio <sup>2</sup> ( $F_r k_2/k_1$ )	Experimental ( $t_p/t_s$ )	Theory Eq. A7 <sup>3</sup> ( $t_p/t_s$ )
200-ppm xanthan	3.1-3.2	0.28-0.29	$3.41 \pm 0.85$ (7 trials)	.4
	8.3-9.8	0.74-0.88	$1.12 \pm 0.16$ (7 trials)	$1.15 \pm 0.16$
1000-ppm xanthan	18.4-33.2	1.0	$0.47 \pm 0.06$ (4 trials)	$0.53 \pm 0.08$
2000-ppm xanthan	41.2-117	1.0	$0.20 \pm 0.07$ (7 trials)	$0.33 \pm 0.07$

1. Since xanthan solutions are highly shear-thinning,  $F_r$  values varied during injection - especially for the most concentrated polymer solutions
2. When the displacement is viscous *overstable*, this quantity is set to unity
3. Parameter  $\omega = 2/3$
4. Unphysical results are obtained when  $(F_r k_2/k_1 + 1) F_r^{1-\omega} < 2$  in Eq. A7

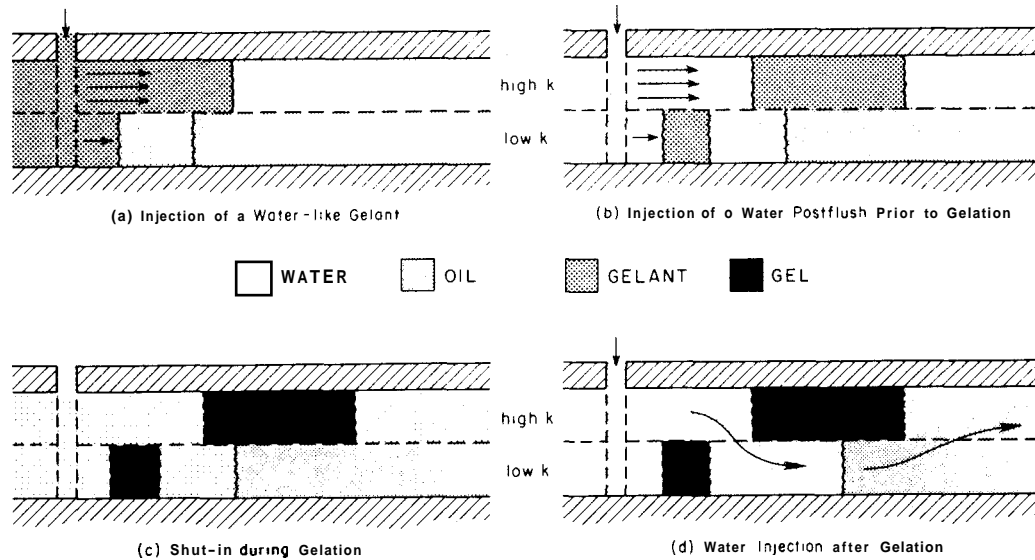


Figure 1: Schematic view of the gelant placement, postflush, gel formation and subsequent water flows in a profile control treatment in the presence of crossflow.

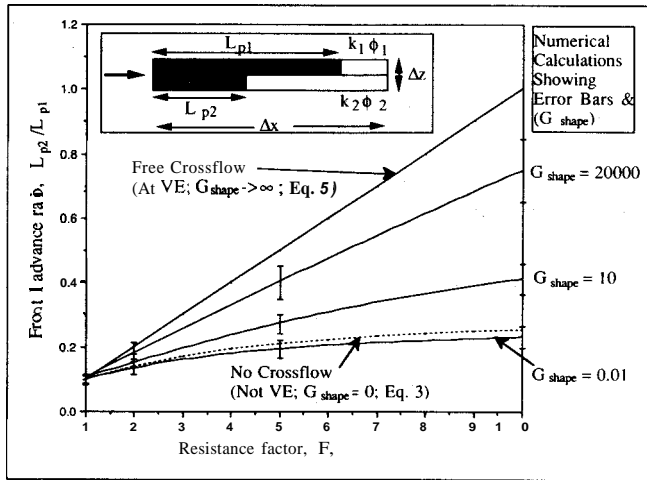


Figure 2: Relative depth of penetration,  $L_{p2}/L_{p1}$ , as a function of  $F_r$  both with and without crossflow between layers

Figure 4: Numerical simulation demonstrating viscous fluid crossflow in a two layer system as a function of the injected fluid viscosity ( $k_1/k_2 = 10$ ;  $k_2 = k_x$ ;  $\Delta x/\Delta z = 10$ ;  $G_{shape} = 100$ )

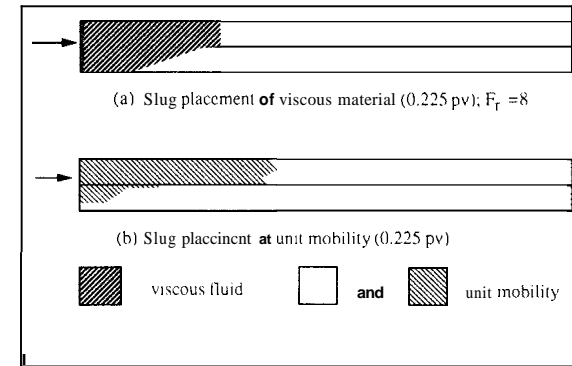
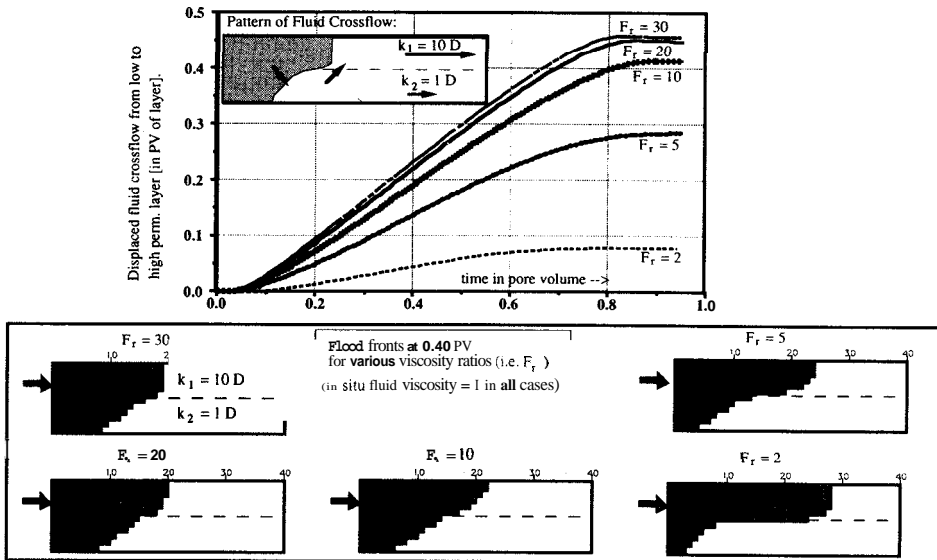


Figure 3: Comparison of (a) a viscous overstable slug placement with (b) a unit mobility case in a two layer stratified headpack:  $k_1/k_2 = 5$ ;  $F_r = 8$  (Pack 1; Table 1)

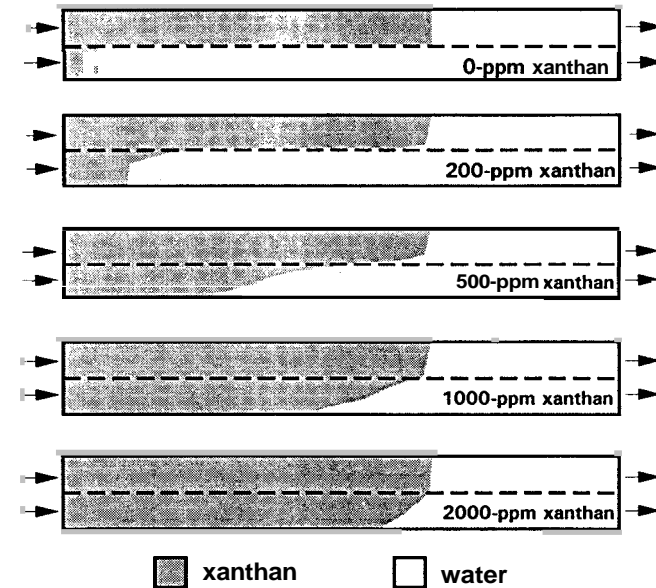


Figure 5: Crossflow in a two layer headpack during displacement of water by xanthan solutions;  $k_1/k_2 = 1.2$ ;  $F_r$  = varying (Pack 2, Table 1).

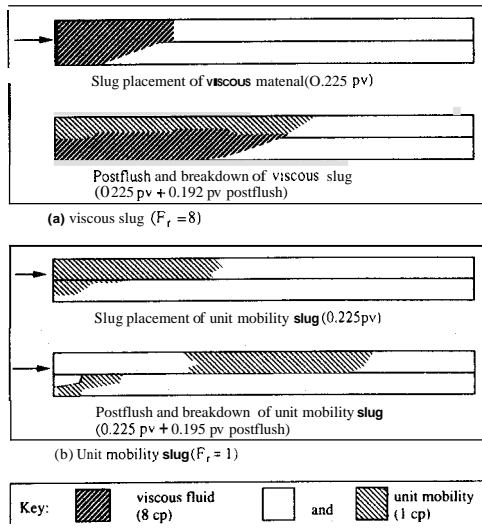


Figure 6 Comparison of the placement/postflush period for a viscous overstable and a unit mobility slug:  $k_1/k_2 = 5$ ,  $F_r = 8$  (Pack 1: Table 1).

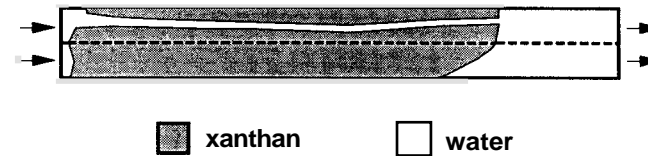


Figure 7: An example of the fingering of water through a bank of 2000 ppm xanthan; fingers form in the high permeability layer (Pack2; Table 1).

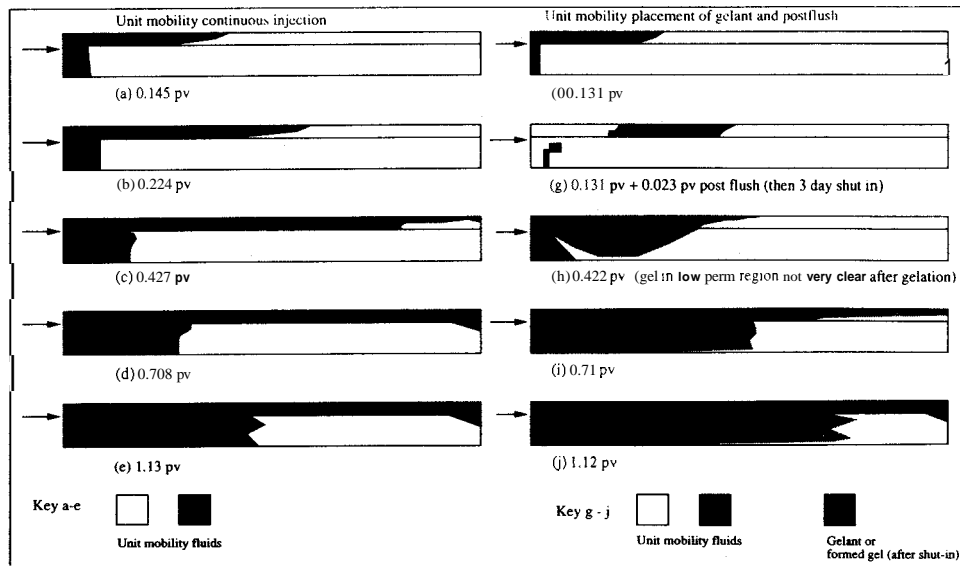


Figure 8: Experimental comparison of a unit mobility continuous displacement with a corresponding unit mobility gelant treatment using a model fluid system which subsequently sets in the pack (see text);  $k_1/k_2 = 5$ ; (Pack 3: Table 1).

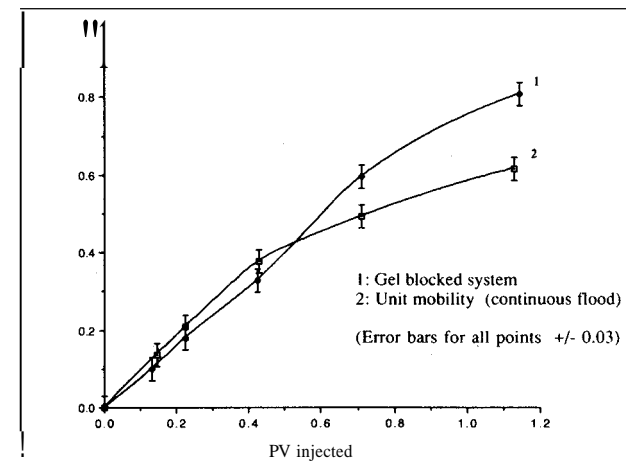


Figure 9: Recovery vs. total pore volume injected for the experimental floods in Fig. 8 comparing the recovery for a gel treatment with that of the "untreated" system in a unit mobility continuous displacement (Error bars for all points +/- 0.03)

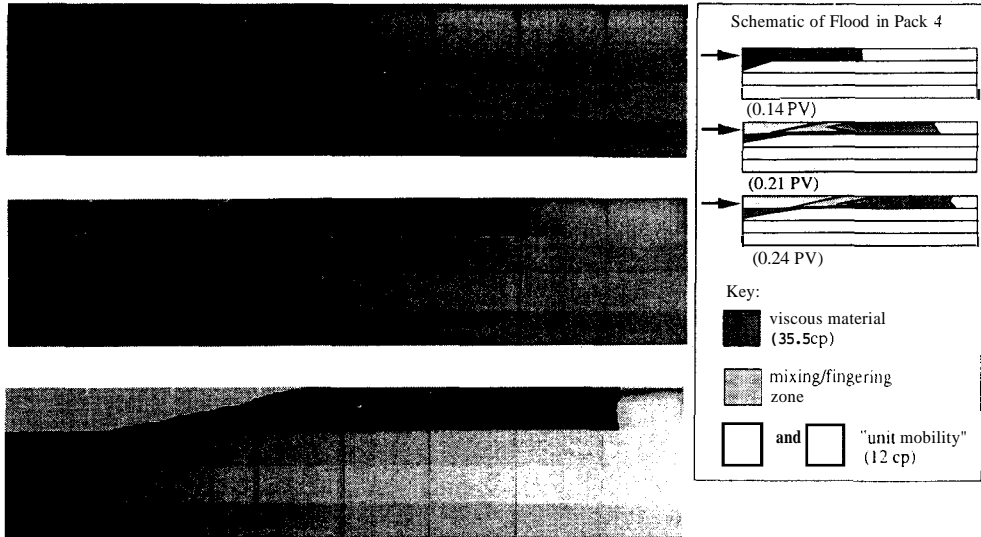


Figure 10: Images from the viscous slug placement in Pack 4 (Table 1) with  $F_r = 2.96$ ; interpretation shown inset

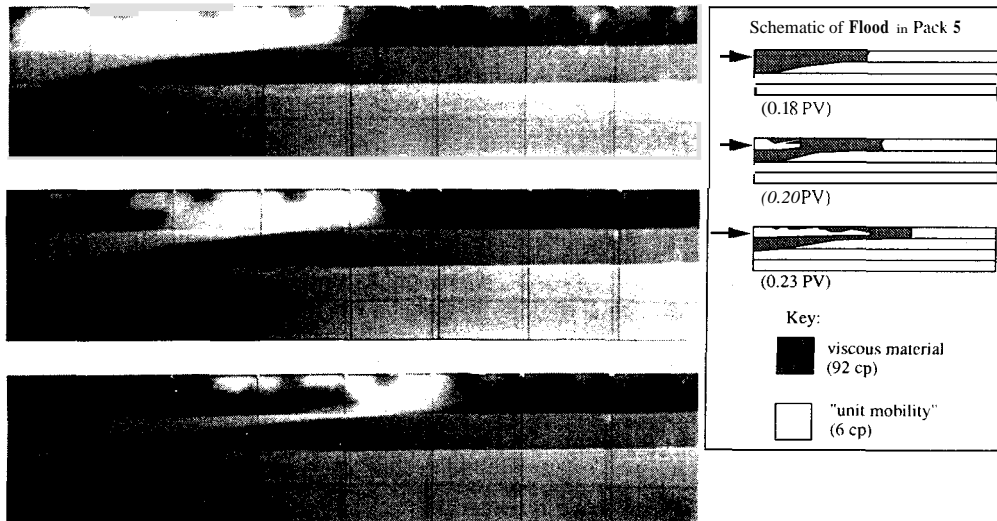


Figure 11: Images from the viscous slug placement in Pack 5 (Table 1) with  $F_r = 15.3$ ; interpretation shown inset

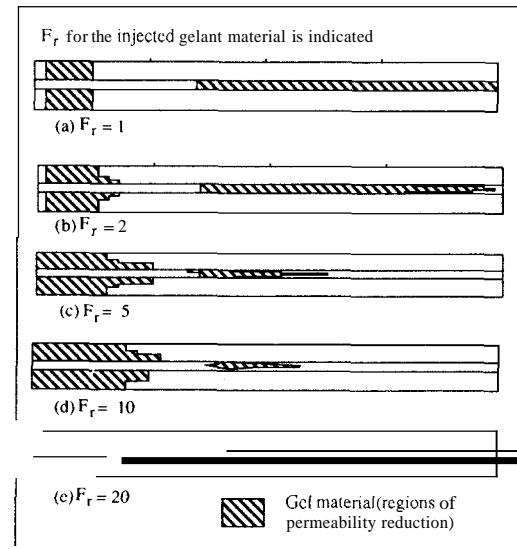


Figure 12: Calculated position of the gelant from numerical simulation for a simple three-layer system with  $k_1/k_2 = 10$  for a range of gelant viscosities; 0.2 PV viscous slug followed by 0.1 PV of brine postflush. Region of reduced permeability (see text) is shown shaded.

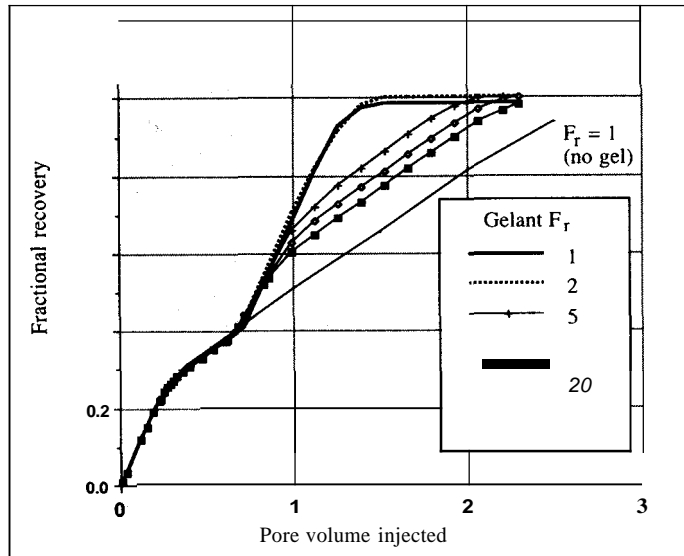


Figure 13: Recovery performance in the stratified three layer system in Fig. 12 for various gelant slug viscosities compared with the continuous unit mobility flood.

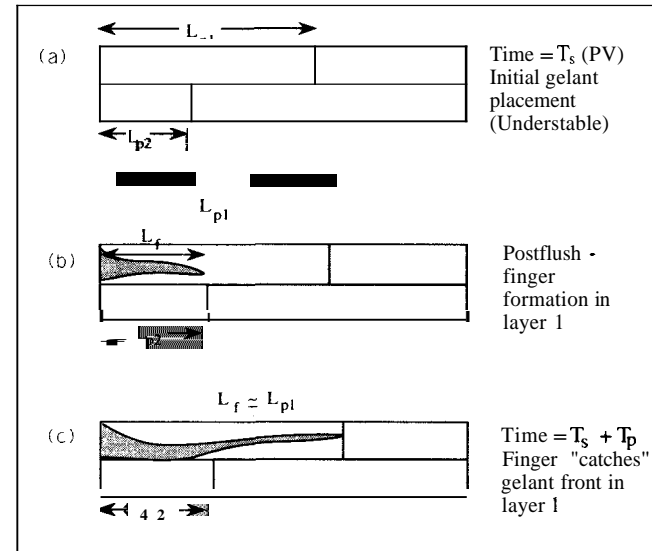


Figure 14: Schematic view of the breakdown of a viscous slug by fingering in a layered system

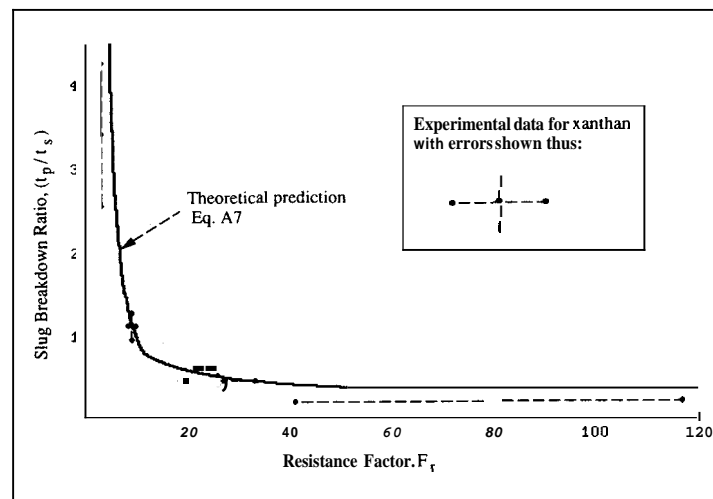


Figure 15: Comparison of experimental and theoretical dimensionless slug breakdown ratio for viscous fingering through xanthan slugs in layered systems: Eq. A7 with  $\omega = 2/3$ , Pack 2,  $k_1/k_2 = 11.2$ , see data in Table 4.